Published online 21 October 2009

Nucleic Acids Research, 2010, Vol. 38, No. 1 ***117–130***
doi:10.1093/nar/gkp863

Novel recognition motifs and biological functions of the RNA-binding protein HuD revealed by genome-wide identification of its targets

Federico Bolognani[1], Tania Contente-Cuomo[2] and Nora I. Perrone-Bizzozero[3,*]

[1]Cell Biology and Physiology, University of New Mexico HSC, Albuquerque, NM, USA, [2]Translational Genomics (T-Gen), Phoenix, AZ, USA and [3]Department of Neurosciences, University of New Mexico School of Medicine, 1 University of New Mexico, MSC08 4740, Albuquerque, NM 87131, USA

Received May 22, 2009; Revised September 24, 2009; Accepted September 28, 2009

ABSTRACT

HuD is a neuronal ELAV-like RNA-binding protein (RBP) involved in nervous system development, regeneration, and learning and memory. This protein stabilizes mRNAs by binding to AU-rich instability elements (AREs) in their 3′ unstranslated regions (3′ UTR). To isolate its *in vivo* targets, messenger ribonucleoprotein (mRNP) complexes containing HuD were first immunoprecipitated from brain extracts and directly bound mRNAs identified by subsequent GST-HuD pull downs and microarray assays. Using the 3′ UTR sequences of the most enriched targets and the known sequence restrictions of the HuD ARE-binding site, we discovered three novel recognition motifs. Motifs 2 and 3 are U-rich whereas motif 1 is C-rich. *In vitro* binding assays indicated that HuD binds motif 3 with the highest affinity, followed by motifs 2 and 1, with less affinity. These motifs were found to be over-represented in brain mRNAs that are upregulated in HuD overexpressor mice, supporting the biological function of these sequences. Gene ontology analyses revealed that HuD targets are enriched in signaling pathways involved in neuronal differentiation and that many of these mRNAs encode other RBPs, translation factors and actin-binding proteins. These findings provide further insights into the post-transcriptional mechanisms by which HuD promotes neural development and synaptic plasticity.

INTRODUCTION

mRNA stability is now recognized as a critical post-transcriptional mechanism controlling the expression of a large number of mammalian genes. Transcript stability is dictated by *cis*-acting elements, mostly localized in the 3′ untranslated region (3′ UTR) and by the activity of *trans*-acting factors, such as microRNAs (miRNAs) and RNA-binding proteins (RBPs) (1–3). The best characterized *cis*-acting instability-conferring sequence is the AU-rich element [ARE; (4,5)]. These sequences were originally described in short-lived transcripts encoding cytokines, oncogenes, and growth factors, however, mRNAs for proteins serving a wide variety of functions have been recently identified as containing AREs (6). AREs regulate mRNA decay by interacting with ARE-binding proteins that either trigger mRNA decay [e.g. KH homology splicing regulatory protein (KSRP), tristetraprolin (TTP), AUF1 and butyrate response factor 1 (BRF1)] or stabilization (e.g. Hu proteins) (1,2). In addition to AREs, other elements regulating mRNA stability have been described. For example, a GU-rich element (GRE) that is a target of the CUG-binding protein 1 (CUGBP1/EDEN-BP) was recently identified in the 3′ UTR of many unstable mRNAs (7–9). Furthermore, a few reports have shown the presence of instability sequences in the 5′ UTR (10) and coding region (11); yet, how common these non-3′ UTR localizations are is presently unclear.

Hu proteins are human homologs of Drosophila embryonic lethal abnormal vision (ELAV, 12) and the best-known mRNA stabilizing factors. There are four mammalian ELAV-like/Hu proteins. While HuC and HuD are exclusively expressed in neurons, HuB is found in neurons and gonads, and HuR is ubiquitously expressed in all tissues. Amongst the *trans*-acting factors that mediate mRNA stabilization, HuD has been shown to play a vital role in neural development and brain physiology, as recently demonstrated by mouse lines either lacking or over-expressing the protein (13–16). HuD knock-out mice show neurogenesis deficits as well as abnormal motor control and development of cranial nerves (13). Over-expression of HuD in transgenic mice leads to alterations in hippocampal physiology and

*To whom correspondence should be addressed. Tel: +1 505 272 1165; Fax: +1 505 272 8082; Email: nbizzozero@salud.unm.edu

deficits in several spatial and associative learning and memory tasks (16,17). In addition to its role in the central nervous system, HuD has also been associated with axonal re-growth after peripheral nerve injury (18,19). Overall, these studies demonstrate that HuD is required for normal neural development, nerve regeneration and synaptic plasticity (20,21).

At the molecular level HuD binds to several unstable mRNAs and as a result of this interaction the target transcripts are stabilized (22,23). HuD has three RNA-recognition motifs (RRM) and we have previously shown that the first two RRMs of the HuD protein are necessary for binding to GAP-43 mRNA, one of HuD's best characterized targets (22). However, these domains by themselves are not sufficient to stabilize GAP-43 mRNA in neuronal cells (24) as it also requires the interaction of RRM III with long poly(A) tails (23). Besides GAP-43, other mRNAs such as N-myc, AChE, tau, neuroserpin and MARCKS mRNAs were shown to interact with HuD *in vitro* and *in vivo* (2). However, the majority of HuD's targets in neurons remain to be elucidated.

Several recent studies identified mRNAs associated with mRNPs containing different RBPs using RNA immunoprecipitation (RIP)-Chip assays, a procedure known as ribonomics (25–28). As mRNPs may represent eukaryotic post-transcriptional operons (29), this procedure provides an important tool for defining the biological function of these RNA–protein complexes. HuD was shown to bind other RBPs including the neuronal ELAV-like protein HuB (30), TAP/NXF1, the primary mRNA export receptor (31) and the IGF-2 mRNA-binding protein IMP1a (32). Therefore, in order to determine which of the mRNAs in HuD-containing mRNPs are directly interacting with this RBP, in the present study we combined the original ribonomics protocol with subsequent *in vitro* pull down assays with GST-HuD. Using this two-step isolation method, nearly 700 new HuD targets were identified. The 3′ UTRs of these targets were then used to discover new HuD-binding motifs and identify the biological and molecular pathways regulated by this protein. As a group, HuD target mRNAs encoded proteins involved in several signaling pathways required for neural differentiation and synaptic remodeling. Interestingly, many of the proteins encoded are also RBPs and translation factors, suggesting that HuD is part of a complex post-transcriptional gene regulatory network.

MATERIALS AND METHODS

mRNA immunoprecipitation

mRNPs containing HuD were immunoprecipitated using the ribonomics protocol described by Tenenbaum and colleagues (25,26). Briefly, forebrain tissue from the HuD transgenic mice (16) were homogenized using a Dounce homogenizer in Polysome Lysis Buffer (100 mM KCl, 5 mM $MgCl_2$, 10 mM HEPES pH 7.0, 0.5% Nonidet P-40, 1 mM dithiothreitol, 100 U/ml RNAsin, 0.2% vanadyl ribonucleoside complexes, leupeptin and aprotinin). Lysates were cleared by centrifugation at $14\,000 \times g$ for 10 min at 4°C and frozen at −80°C until use. Protein G-Sepharose beads (Sigma, St. Louis, MO) were coated with anti myc-monoclonal antibody (9B11 mouse mAb, Cell Signaling Technology, Danvers, MA) or non-immune mouse IgG (Sigma, St. Louis, MO) under constant rocking in NT2 buffer [50 mM Tris (pH 7.4), 150 mM NaCl, 1 mM $MgCl_2$ and 0.05% Nonidet P-40] supplemented with 5% BSA. Brain extracts (100 µl) were immunoprecipitated with 50 µl of coated beads in 850 µl of NT2 buffer supplemented with 8 units of RNAsin, 1 mM vanadyl ribonucleoside complexes, 1 mM DTT and 15 mM EDTA for 2 h at room temperature under constant rocking. After beads were washed six times with ice-cold NT2 buffer, proteins were digested with proteinase K and mRNAs purified by phenol–chloroform extraction and ethanol precipitation.

GST HuD pull down assays

Recombinant GST-HuD protein was prepared from BL21 *Escherichia coli* transformed with pGEX-2T-HuD plasmid as described previously (23,33). Briefly, BL21 cells were induced with IPTG and lysed by sonication in Fast Break Cell Lysis Reagent (Promega, Madison, WI) supplemented with Halt Protease inhibitor (Pierce, Rockford, IL) and RQ1 DNase (Promega, Madison, WI). After centrifugation for 15 min at 4°C at $27\,000 \times g$, the supernatant was incubated for 1 h at 4°C with MagneGST Glutathione Particles (Promega, Madison, WI). Beads were washed with Binding/Wash buffer (Promega, Madison, WI) and incubated with 600 ng of amplified RNA from the previous ribonomics step for 30 min at 4°C in binding buffer (10 mM HEPES, 3 mM $MgCl_2$, 40 mM KCl, 1 mM DTT, 400 U of RNase out and 5% glycerol). After incubation and washes with binding buffer without glycerol, RNA was extracted as described above.

mRNA amplification and array hybridization

Total RNA (10 ng) from the first and second purification steps was converted to double-stranded cDNA using the GeneChip® Expression 3′-Amplification Two-Cycle Target Labeling and Control Reagents Kit (Affymetrix, Santa Clara, CA) according to manufacturer's protocols. The resulting cDNA was used for the *in vitro* synthesis of biotin-labeled cRNA using the GeneChip® IVT Labeling Kit (Affymetrix). cRNA was cleaned using the GeneChip® Sample Cleanup Module and fragmented into 35–200 base pair fragments using a magnesium acetate buffer (Affymetrix). In total, 6.5 µg of labeled cRNA was hybridized to Affymetrix GeneChip® Mouse Genome 430 2.0 for 16 h at 45°C. The arrays were washed and stained according to the manufacturer's recommendations using the GeneChip Fluidics Station 450 (Affymetrix). Each array was scanned using the GeneChip® Scanner 3000 (Affymetrix) and globally scaled to 150 using the Affymetrix GeneChip® Operating Software (GCOS v1.4).

Microarray analysis

Samples were run in triplicates. For target identification, raw data files from the Affymetrix arrays were normalized

to the RNA levels used for cRNA synthesis and $\log_2$ of the normalized values were used to calculate the enrichment ratios of HuD IP versus IgG IP and GST-HuD versus GST pull downs. Probes with absent calls in at least two out of three replicates in the HuD IP and the GST-HuD pull down chips but not in the controls (IgG IP and GST pull down) were excluded from the analysis and the average enrichment for each probe was used for statistical analyses. A similar analysis was used to identify mRNAs that were up-regulated in the brains of HuD transgenic overexpressor mice (HuD-Tg). Briefly, mRNAs from three HuD-Tg mice and three control (non-transgenic) littermates were analyzed by Affymetrix 430 2.0 chips and mRNAs that had 'present' calls and were significantly upregulated ($P < 0.05$), as determined using GeneSpring 9.0 (Agilent Technologies, Santa Clara, CA), were used for HuD motif analyses. In addition, we generated a list of all the mRNA expressed in mouse forebrain using transcripts from control forebrains with 'present' calls and raw expression values more than 100, which corresponds to twice the background level. This set, which consisted of 17 010 transcripts corresponding to 9757 genes, was used as reference for HuD target analyses (see below).

Sequence analysis

The 3′ UTR, coding region (CR) and 5′ UTR sequences of HuD targets, the genes in the Affymetrix 430 2.0 chip, the mouse forebrain set described above and all the genes available in the Ensembl database were downloaded from Ensembl BioMart, release 49, Mus musculus genes NCBIM37 (http://www.ensembl.org/biomart/index.html). The datasets were made non-redundant based on gene ID using our own Perl scripts. If more than one sequence was available for a gene, the longest was chosen for further analysis. 3′ UTR nucleotide composition and length, presence of each ARE subtype, and U stretches were analyzed using custom scripts written in Perl v5.8.8 and BioPerl 1.5.2 modules (http://www.bioperl.org), which are available upon request. Differences between datasets were analyzed by two by two contingency tables with Chi-square test using the R statistical package version 2.7.1.

Motif search and analysis

Bioinformatics analyses for HuD-binding motifs considered both the 3′ UTR sequences of the 72 most enriched targets and the restrictions imposed by the three-dimensional structure of the complex between the first two RRMs in HuD and two different Class I and II AREs (34). The 3′ UTR sequences of the 72 most enriched HuD targets downloaded from Ensembl BioMart and 25 nucleotide (nt) long fragments containing the consensus binding sequence YUNNYUY in the middle were extracted. Since the YUNNYUY sequence is not very restrictive, One-thousand seven-hundred thirty-five fragments were obtained. These sequences were used as a training set for motif search using MEME software [http://meme.sdsc.edu/meme; (35,36)]. A diagram of the implemented motif search strategy is shown in Figure 3A. Probability matrices of the new HuD-binding motifs were represented graphically using WebLogo [http://weblogo.berkeley.edu/; (37)]. For analyzing the frequency of each new HuD-binding motif in the different datasets and the location of each motif, we used a Perl script that searches for the following regular expressions (allowing one mismatch): [CG][CT][CT]TC[CT][CT]TC[TC]C[TC]C, [TG]TTTGTTT[TG][GT]TTT, and TTTTTTTTT[TA]AAA, for motifs 1, 2 and 3, respectively. Differences between datasets were analyzed by two by two contingency tables with Chi-square test using the R statistical package version 2.7.1.

Nitrocellulose filter binding assay

Ribo-oligoribonucleotides (Integrated DNA Technologies, Coralville, IA) were end-labeled with P^{32}gamma-ATP from MP Biomedicals using polynucleotide kinase (New England Biolabs). Labeled oligoribonucleotides were purified using mini Quick Spin Columns (Roche Applied Sciences, Indianapolis, IN) and used immediately for *in vitro* binding assays. Reaction mixtures (20 µl) contained 50 mM Tris (pH 7.0), 150 mM NaCl, 0.25 mg/ml bovine serum albumin, 0.25 mg/ml tRNA and labeled oligoribonucleotides as indicated. We used 100 ng per reaction of recombinant HuD for motifs 2 and 3, and 600 ng for motif 1. After 20 min incubation at 37°C, the mixtures were diluted 1:6 with wash buffer (20 mM Tris–HCl pH 7.0 and 50 µg/ml tRNA) and filtered through a nitrocellulose membrane using a dot blot apparatus. Membranes were washed twice with wash buffer. To determine the non-specific binding, similar reactions were carried out in parallel with a 100 molar excess of unlabeled oligoribonucleotide. Bound radioactivity was determined using a phosphor-imager (Personal Molecular Imager, BioRad). Serial dilutions of each labeled oligonucleotide were blotted directly onto the membrane and used to measure total radioactivity.

Gene ontology analysis

The Gene Ontology Tree Machine [GOTM, http://bioinfo.vanderbilt.edu/gotm/, (38)] and WebGestalt [http://bioinfo.vanderbilt.edu/webgestalt, (39)] programs were used for these studies. The frequencies and numbers of HuD targets in each gene ontology category were calculated and compared to those in the mouse genome. A hypergeometric distribution test was used to calculate the statistical significance of the observed (HuD targets dataset) over the predicted (genomic) frequency. *P*-values smaller than 0.01 were considered statistically significant and only gene ontology categories with more than three genes in the HuD targets dataset were considered. Biological pathways associated with HuD targets were identified using the links to the Kyoto Encyclopedia of Genes and Genomes (KEGG) available thorough GOTM and WebGestalt. MetaCore pathway analysis software was also used (GeneGO, Encinitas, CA).

RESULTS

Identification of HuD targets

HuD expression is critical for normal brain development and maturation and thus the identification of the repertoire of HuD's targets is an important first step towards the characterization of the molecular processes regulated by this RBP. In this study, we used two consecutive purification steps to isolate HuD-bound mRNAs (Figure 1). First, neuronal HuD-containing mRNPs were purified from brain extracts of HuD overexpressor mice (14) by immunoprecipitation (IP). Since none of the commercially available HuD antibodies worked well for the IP step, antibodies against the myc-tag present in the HuD transgene were used instead to pull down the protein. Validating the IP step we found that GAP-43 and neuroserpin mRNAs, two of the known targets of HuD, were enriched close to 7- and 70-fold, respectively, in the HuD IP (Supplementary Figure S1). Following mRNA extraction and oligo-dT-T7 directed linear amplification direct targets were subsequently enriched by affinity purification using GST-HuD protein (Figure 1). After each step of purification, mRNAs were isolated, subjected to a two-round linear amplification and hybridized to Affymetrix 430 2.0 arrays.

Enrichments were calculated by dividing the signal of each probe set in the HuD IP or GST-HuD pull down by the signal of the same probe in the non-immune IgG IP or control GST pull down, respectively. The mean enrichment of mRNAs in the IP step was 2-fold and the use of the GST-HuD step increased this value to 12-fold. As indicated above, one possible explanation for this finding is that many of the mRNAs immunoprecipitated in the first step may be interacting with other proteins in the mRNP. Also, since this is the first time that the RIP-Chip protocol was used for the analyses of Hu protein targets in the brain and Affymetrix arrays were probed with equal amounts of control and HuD IP RNA, the global enrichment in the IP step was lower than that observed for other Hu proteins in cultured cells (25,40). Nevertheless, analyses of the mRNAs enriched in the brain HuD-IP step with those associated with HuR in Jurkat cells (40) resulted in similar enrichment plots for both sets of mRNAs (data not shown). Overall, we found that 5412 probes corresponding to 3529 known genes and expressed sequence tags (ESTs) showed more than 2-fold enrichment after the first step and 1189 probes (1034 genes) had *z*-scores above 1.5 after the two consecutive isolation steps. Seven hundred probes (673 genes) met both enrichment criteria and were operationally defined as putative HuD targets. Table 1 shows the 70 most enriched mRNAs in the dataset and the complete list of 700 probes is shown in Supplementary Table S1. Although not all the previously reported targets of HuD were included in this dataset, we found that all of them were enriched at least 3-fold after the second purification step and/or contained one of the three RNA-binding motifs described below (Figure 3, Table 3).

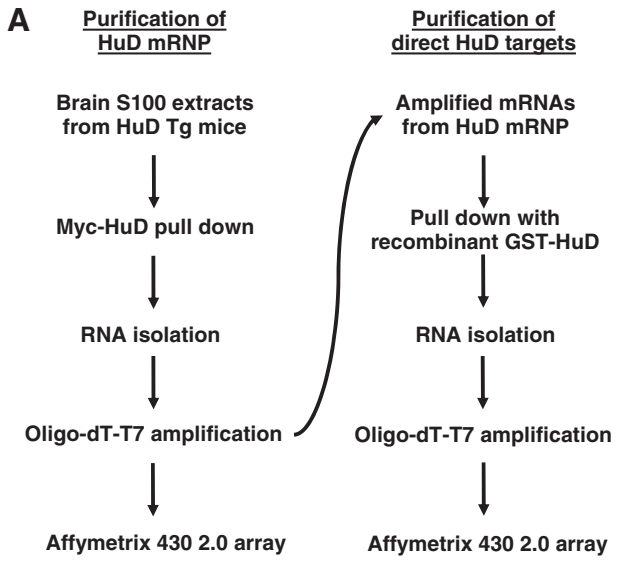

Figure 1. Identification of HuD target mRNAs. Experimental strategy implemented for analyzing HuD target mRNAs at genomic scale. The flow chart shows the two sequential steps used for the identification of HuD targets.

3′ UTR sequence characteristics of HuD targets

The 5′ UTR, coding region (CR), and 3′ UTR sequences of all the mRNAs in the HuD target set, mouse genome, and Affymetrix 430 2.0 chip were extracted from Ensembl BioMart. Since ~50% of the genome is expressed in the brain, we generated a set of forebrain-expressed mRNAs (see 'Materials and Methods' section) and used this set of transcripts to compare with HuD targets as well. As shown in Table 2, the average 3′ UTR length in HuD target mRNAs is surprisingly longer than in then genome, the Affymetrix chip and the forebrain set (HuD targets: 1909 nt versus 1121 in mouse genome, 1142 in the chip and 1325 in forebrain transcripts). Also, we found that the forebrain set had slightly longer 3′ UTRs and slightly shorter 5′ UTRs than the genome and chip sets. The increased 3′ UTR length of forebrain mRNAs relative to the entire mouse transcriptome is consistent with a previous report showing a positive correlation between the 3′ UTR length of mRNAs and their brain-specific expression (41) and with the observations that some brain-expressed mRNAs have longer 3′ UTRs than their counterparts in other tissues (42–44). Regarding the relative abundance of all four nucleotides in the sequence, we found that the 3′ UTRs in the HuD target dataset are slightly more U-rich than the three reference datasets. No difference between the *Mus musculus* genome and the genes present in the Affymetrix chip were observed, demonstrating that the Affymetrix 430 2.0 chip contains an unbiased representation of all mouse genes. Furthermore, aside for small differences in the lengths of the 5′ and 3′ UTRs, the properties of forebrain transcripts did not differ significantly from those of the other two reference datasets (Table 2, Figure 2).

Subsequent analyses examined the frequency of known mRNA instability elements in the 3′ UTRs of mRNAs in three reference transcripts sets and the HuD target

Table 1. Partial list of HuD targets

Probe set ID	Fold enrichment	Gene symbol	Description	Ensembl
1438554_x_at	19.43	Eif4h	Eukaryotic translation initiation factor 4H	ENSMUSG00000040731
1452833_at	19.42	Rapgef2	Rap guanine nucleotide exchange factor (GEF) 2	ENSMUSG00000062232
1424358_at	19.16	Ube2e2	Ubiquitin-conjugating enzyme E2E 2 (UBC4/5 homolog, yeast)	ENSMUSG00000058317
1434277_a_at	19.08	Ypel2	Yippee-like 2 (Drosophila)	ENSMUSG00000018427
1416313_at	18.85	Mllt11	Myeloid/lymphoid or mixed-lineage leukemia (trithorax homolog, Drosophila); translocated to, 11	ENSMUSG00000053192
1434310_at	18.78	Bmpr2	Bone morphogenic protein receptor, type II (serine/threonine kinase)	–
1429839_a_at	18.63	Yaf2	YY1 associated factor 2	ENSMUSG00000022634
1435521_at	18.5	Msi2	Musashi homolog 2 (Drosophila)	ENSMUSG00000069769
1457248_x_at	18.47	Hsd17b7	Hydroxysteroid (17-beta) dehydrogenase 7	ENSMUSG00000026675
1435807_at	18.46	Cdc42	Cell division cycle 42 homolog (*S. cerevisiae*)	ENSMUSG00000006699
1416767_a_at	18.45		RIKEN cDNA 1110003E01 gene	ENSMUSG00000037822
1433519_at	18.43	Nucks1	Nuclear casein kinase and cyclin-dependent kinase substrate 1	–
1450021_at	18.38	Ubqln2	Ubiquilin 2	ENSMUSG00000050148
1437457_a_at	18.38	Mtpn	Myotrophin	ENSMUSG00000029840
1416082_at	18.32	Rab1	RAB1, member RAS oncogene family	ENSMUSG00000020149
1448100_at	18.31		RIKEN cDNA 4833439L19 gene	ENSMUSG00000025871
1447776_x_at	18.29	Rab6	RAB6, member RAS oncogene family	ENSMUSG00000030704
1432198_at	18.29		RIKEN cDNA A230083H22 gene	ENSMUSG00000039126
1448504_a_at	18.28	Cbx3	Chromobox homolog 3 (Drosophila HP1 gamma)	ENSMUSG00000029836 ENSMUSG00000059647
1415971_at	18.23	Marcks	Myristoylated alanine rich protein kinase C substrate	ENSMUSG00000069662
1426776_at	18.21	Wasl	Wiskott–Aldrich syndrome-like (human)	ENSMUSG00000029684
1433540_x_at	18.16	Ppp1cb	Protein phosphatase 1, catalytic subunit, beta isoform	ENSMUSG00000014956
1426401_at	18.15	Ppp3ca	Protein phosphatase 3, catalytic subunit, alpha isoform	ENSMUSG00000028161
1419112_at	18.12	Nlk	Nemo like kinase	ENSMUSG00000017376
1423895_a_at	18.11	Cugbp2	CUG triplet repeat, RNA-binding protein 2	ENSMUSG00000002107
1423220_at	18.07	Eif4e	Eukaryotic translation initiation factor 4E	ENSMUSG00000028156
1458351_s_at	18.06	Klhl2	Kelch-like 2, Mayven (Drosophila)	ENSMUSG00000031605
1440270_at	18.05	Fgf12	Fibroblast growth factor 12	ENSMUSG00000022523
1434082_at	18.04	Pctk2	Serine/threonine-protein kinase PCTAIRE-2	ENSMUSG00000020015
1434232_a_at	18.04		RIKEN cDNA 2610030H06 gene	ENSMUSG00000073131
1428473_at	18.03	Ppp3cb	Protein phosphatase 3, catalytic subunit, beta isoform	ENSMUSG00000021816
1448184_at	18.03	Fkbp1a	FK506-binding protein 1a	ENSMUSG00000032966
1447669_s_at	18.02	Gng4	Guanine nucleotide binding protein (G protein), gamma 4 subunit	ENSMUSG00000021303
1428970_at	18.01	Nat13	N-acetyltransferase 13	ENSMUSG00000022698
1437585_x_at	17.99	Zfp161	Zinc finger protein 161	ENSMUSG00000049672
1419246_s_at	17.99	Rab14	RAB14, member RAS oncogene family	ENSMUSG00000026878
1438007_at	17.94		Expressed sequence AI851790	ENSMUSG00000044071
1424852_at	17.87	Mef2c	Myocyte enhancer factor 2C	–
1436452_x_at	17.82	Tmed2	Transmembrane emp24 domain trafficking protein 2	ENSMUSG00000029390 ENSMUSG00000074460
1428416_at	17.79		RIKEN cDNA 3110050N22 gene	ENSMUSG00000043542
1417377_at	17.78	Cadm1	Cell adhesion molecule 1	ENSMUSG00000032076
1433521_at	17.75	Ankrd13c	Ankyrin repeat domain 13c	ENSMUSG00000039988
1433751_at	17.73	Slc39a10	Solute carrier family 39 (zinc transporter), member 10	ENSMUSG00000025986
1424215_at	17.72	Fundc1	FUN14 domain containing 1	ENSMUSG00000025040
1434620_s_at	17.72		RIKEN cDNA 2610024E20 gene	ENSMUSG00000036501
1421323_a_at	17.71	G3bp2	GTPase activating protein (SH3 domain) binding protein 2	ENSMUSG00000029405
1423309_at	17.7	Tgoln1	*Trans*-golgi network protein	ENSMUSG00000056429
1426864_a_at	17.7	Ncam1	Neural cell adhesion molecule 1	ENSMUSG00000039542
1424683_at	17.67		RIKEN cDNA 1810015C04 gene	ENSMUSG00000022270
1418067_at	17.65	Cfl2	Cofilin 2, muscle	ENSMUSG00000062929
1437801_at	17.62	Morf4l1	Mortality factor 4 like 1	ENSMUSG00000062270
1428537_at	17.62	Csnk1a1	Casein kinase 1, alpha 1	ENSMUSG00000024576
1419971_s_at	17.61	Slc35a5	Solute carrier family 35, member A5	ENSMUSG00000022664
1417410_s_at	17.61	Prkci	Protein kinase C, iota	ENSMUSG00000037643
1417411_at	17.61	Nap1l5	Nucleosome assembly protein 1-like 5	ENSMUSG00000029804
1418436_at	17.6	Stx7	Syntaxin 7	ENSMUSG00000019998
1422748_at	17.58	Zeb2	Zinc finger E-box binding homeobox 2	ENSMUSG00000026872
1434820_s_at	17.57	Pkig	Protein kinase inhibitor, gamma	ENSMUSG00000035268
1415911_at	17.57	Impact	Imprinted and ancient	ENSMUSG00000024423
1454976_at	17.55	Sod2	Superoxide dismutase 2, mitochondrial	ENSMUSG00000006818
1433986_at	17.52		cDNA sequence BC024659	–
1437016_x_at	17.46	Rap2c	RAP2C, member of RAS oncogene family	ENSMUSG00000050029
1434106_at	17.46	Epm2aip1	EPM2A (laforin) interacting protein 1	ENSMUSG00000046785
1416008_at	17.45	Satb1	Special AT-rich sequence binding protein 1	ENSMUSG00000023927

(continued)

Table 1. Continued

Probe set ID	Fold enrichment	Gene symbol	Description	Ensembl
1456177_x_at	17.44	Zfp706	Zinc finger protein 706	ENSMUSG00000062397
1416501_at	17.44	Pdpk1	3-phosphoinositide dependent protein kinase-1	ENSMUSG00000024122
1423684_at	17.44	Hnrpk	Heterogeneous nuclear ribonucleoprotein K	ENSMUSG00000021546
1426924_at	17.4	Rc3h2	Ring finger and CCCH-type zinc finger domains 2	ENSMUSG00000075376
1437288_at	17.38	Impad1	Inositol monophosphatase domain containing 1	ENSMUSG00000066324
1429579_at	17.37		RIKEN cDNA 6330407I18 gene	–

The top 70 most enriched mRNAs of the 700 putative HuD targets. The complete dataset is shown in Supplementary Table S1.

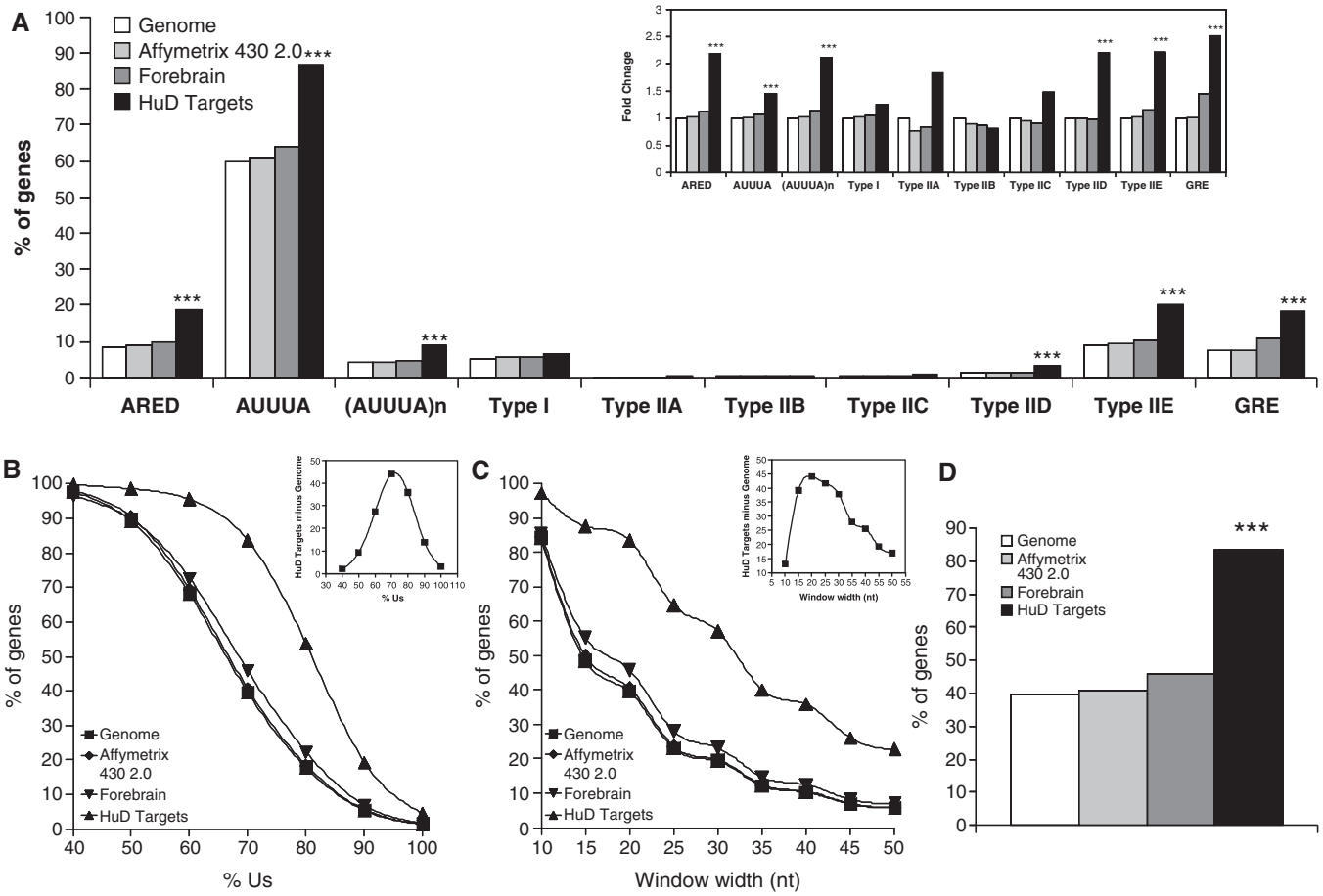

Figure 2. ARE frequency and U content in HuD target genes. (**A**) The presence of the different AREs was analyzed in 3′ UTR sequences of the entire mouse genome (white bars), the genes present in the Affymetrix 430 2.0 chip (light gray bars), a set of forebrain expressed transcripts (dark gray bars) and in the HuD target dataset (black bars). Inset shows the same data normalized to the frequency in the genome. (**B**) Analysis of the percentage of Us in 20 nt long stretches in the 3′ UTRs of the mouse genome, Affymetrix 430 2.0 chip, and HuD targets. Inset shows the difference between HuD targets and mouse genome. (**C**) Percentage of genes with segments of 70% Us as a function of stretch length. Inset shows the difference between HuD targets and mouse genome. (**D**) Frequency of genes with 20 nt long fragments in the 3′ UTR containing at least 70% Us in all the datasets described in panel A. $***P < 0.0001$ after a Chi-square test.

dataset. As shown in Figure 2A, HuD target mRNAs contained significantly higher frequencies of these motifs. Because some of the motifs were very rare, to easily visualize differences the data were normalized to the frequency in the genome (Figure 2A, inset). Of the known instability-conferring sequences, the ARED motif, defined by the following regular expression [AU][AU][AU]U(AUUUA)UUU[AU] with 1 mismatch allowed in the pentamer flanking regions (6) showed an approximate 2-fold enrichment in the HuD target dataset. However, this motif was present in only 20% of the targets. We then examined the presence of the AUUUA pentamer and found a modest but statistically significant increase in the frequency of this sequence in the HuD target dataset. However, given that this motif is present at a high frequency in the genome (~60% of the genes) and a single AUUUA motif by

itself does not constitute an ARE, this sequence is an unlikely candidate for a HuD-recognition motif. The search for ARE motifs was then restricted to overlapping AUUUAs [$(AUUUA)_n$] or AUUUA motifs embedded in a U-rich region (Type I ARE) defined arbitrarily as a 20 nt long stretch with at least 60% U. Overlapping AUUUA pentamers were present at high levels in the HuD target dataset relative to the three reference datasets, but they only accounted for ~10% of the HuD targets. In contrast, type I AREs were not enriched in this set. Analysis of the type II ARE sub-categories proposed by Wilusz and colleagues (1) revealed that that most of these sub-categories were barely represented in the genome. However, sub-categories IID and IIE were more frequent in the HuD target 3′ UTRs. Finally, we searched for the recently reported G-rich element [GRE; (9)] and found that the frequency of GREs was increased among HuD targets. Taking together all the known instability motifs, only 42.48% of all HuD targets could be explained by these sequences suggesting that other elements are involved in HuD target recognition.

The common feature of the previously analyzed ARE sequences is a high U content. Therefore, we performed a detailed analysis of the U content in the 3′ UTR of HuD targets. Figure 2B shows the frequency of 20 nt long stretches with different percentages of U. As the percentage of U increases, the fraction of genes containing these sequences diminishes, however, the HuD target dataset shows a higher number of mRNAs with high U content. When the difference between percentage of genes in the HuD targets and the *Mus musculus* genome was plotted versus percentage of U (Figure 2B, inset), the curve showed a peak at 70% U, suggesting that this percentage is needed for HuD binding. Figure 2C presents a similar analysis, but with a fixed percentage of U set at 70 and variation in the length of the window. The results show an expected decrease in the percentage of genes meeting the criteria as the window gets longer, with the maximum discrimination between HuD targets and the mouse genome at a window length of 20 nts (Figure 2C, inset). Analysis of the frequencies of mRNAs having 20 nt long stretches with 70% U in the 3′ UTR (Figure 2D) revealed that 80% of the HuD targets have this characteristic, a value that was highly significant when compared to the genome, chip and forebrain datasets.

Discovery of new HuD-binding motifs

Because ARE and GRE sequences only explained a fraction of the motifs present in HuD targets and the 20 nt and 70% U criteria is not sequence-specific, subsequent studies searched for new HuD-binding motifs. As shown in Figure 3A, the 3′ UTR sequences of the 72 most enriched HuD targets were used to extract 25 nt long fragments containing the sequence YUNNYUY in the middle. This sequence reflects the minimal binding motif that was derived from modeling studies of the crystal structure of the complex of RRMs I and II in HuD with class I and II AREs (34). Using this filter to remove physiologically irrelevant sequences 1735 fragments were obtained, and this new dataset was used as a training set to search for new HuD-binding motifs. Using a multiple expectation maximization algorithm implemented in the MEME software (35,36), we found three motifs with statistically significant *E*-values, which are represented in Figure 3B by WebLogo graphics (37). Supplementary Table 2 shows the probability matrix for each individual motif. The first motif is pyrimidine-rich with a preponderance of C and a lower U content. This motif is analogous to a C-rich instability element that is present in α-globin and other mRNAs and that is recognized by the poly(C)-binding protein (45,46). The second motif is U-rich with some interspersed Gs, and very similar to the GRE motif (9) and the binding motif of sex-lethal, another homolog of Hu proteins in *Drosophila melanogaster* (47). The last motif is also U-rich with several As and thus is comparable to the classical type I and II AREs.

If these motifs are indeed recognized by HuD, mRNAs carrying these motifs should be present at higher frequency in the HuD target dataset than in the three reference datasets (mouse genome, Affymetrix chip and forebrain transcripts). As shown in Figure 3D the frequency of motif 1 is increased in the 5′ UTR and the 3′ UTR of HuD targets but not in the coding region. Motifs 2 and 3 showed a very similar pattern with highly significant increases in the 3′ UTR and a slight increase in the 5′ UTR and coding regions (Figures 3E and F). Analysis of the distribution of the three motifs (Figure 3C) showed that ~80% (456 out of 572) of the target mRNAs have at least one of the motifs, ~10% have all three motifs in their 3′ UTR and 33% have two motifs. Subsequent analyses mapped the localization of the three motifs in a set of known and novel HuD targets. As shown in Table 3, with the exception of tau, one of the mRNAs identified as a target of HuD in a previous study (32), all the known HuD targets contain at least one of the motifs. Some of the targets such as Musashi 2, N-CAM1, Neuroserpin and CaMkinIIα mRNAs have a large number of motifs while others such as Homer 1, Fkbp1a, PPP1cb and PPP3ca have only one motif per 3′ UTR. In addition, one of the known targets of HuD, the p27 mRNA, contains HuD-binding motifs both in the 5′ and 3′ UTRs, consistent with a role of HuD in translation of this mRNA (48). Altogether these results indicate that the majority of HuD targets can be explained by the presence of these new motifs.

Affinity of HuD for the three motifs

To directly test whether HuD binds these new motifs and to determine the binding affinities we performed *in vitro* binding assays using recombinant protein and synthetic radiolabeled ribo-oligonucleotides corresponding to the most likely sequence of each of the three motifs. The specific binding of HuD to each motif was calculated by subtracting non-specific binding, which was assessed by the addition of 100 times molar excess of unlabeled ribo-oligoribonucleotide. The affinities of recombinant HuD for each motif were then calculated using non-linear regression analyses. As shown in Figure 4, HuD interacts with different affinities with each of the three sequences, with motif 3 showing the highest affinity followed by motif

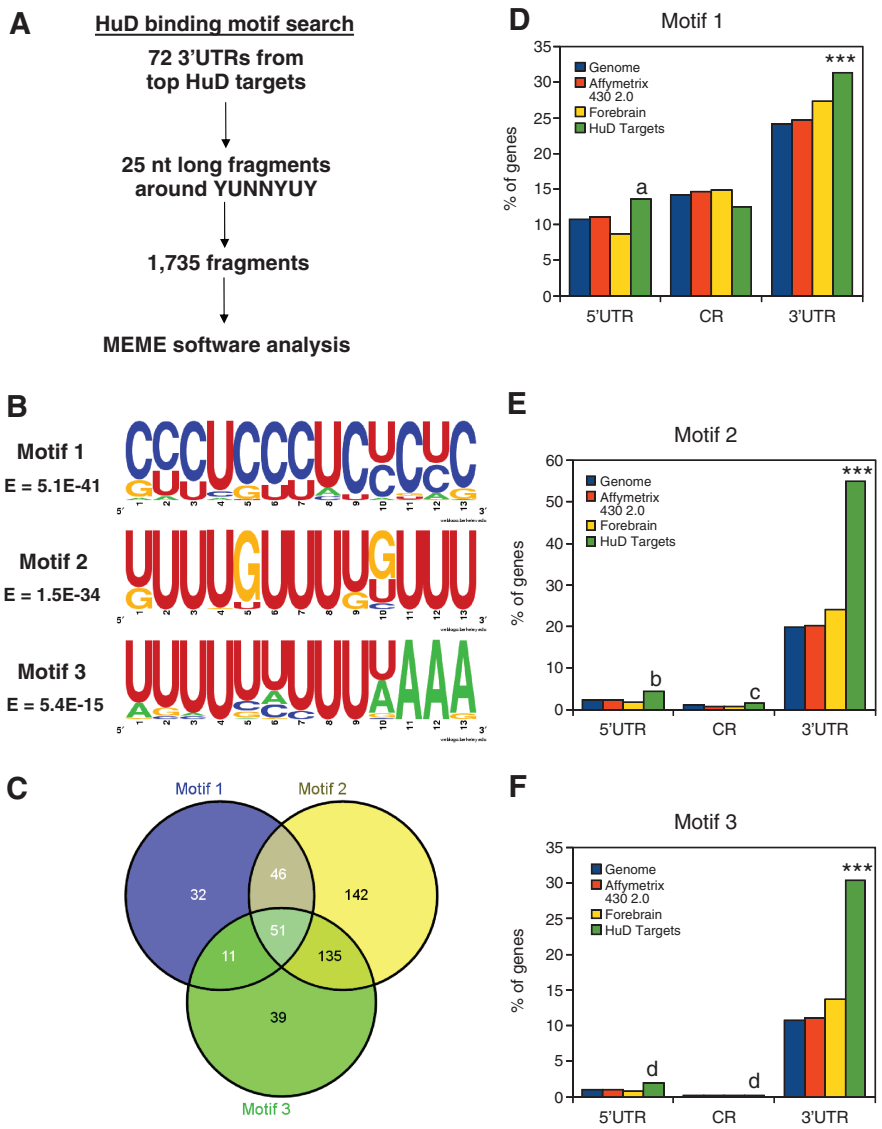

Figure 3. Identification of the HuD-binding motifs. (**A**) Experimental strategy implemented to identify HuD-binding motifs. (**B**) WebLogo representations of the three identified HuD-binding sequences. (**C**) Venn diagram showing the distribution of the three new HuD-binding motifs in the HuD targets. (**D**) Frequency of motif 1 in the 5′ UTR, coding region (CR), and 3′ UTR of mouse genome (blue bars), Affymetrix 430 2.0 chip genes (red bars), forebrain transcripts (yellow bars) and HuD targets (green bars). (**E**) Percentage of presence of motif 2 in the same groups as Panel D. (**F**) Same analysis for motif 3. ***$P < 0.0001$ of HuD targets versus each of the three reference datasets. (a) $P < 0.05$ HuD targets versus genome and forebrain, (b) $P < 0.05$ versus genome, $P < 0.01$ versus chip and $P < 0.0001$ versus forebrain, (c) $P < 0.05$ versus chip and versus forebrain and (d) $P < 0.05$ versus forebrain.

2 and the C-rich motif 1 showing the least affinity (K_d = 2.9 nM motif 3, 6.9 nM motif 2 and 27.3 nM motif 1). Taken together, these data provides experimental validation of the *in silico* identified HuD-binding motifs.

Enrichment of HuD-binding motifs in genes upregulated in HuD-Tg mice

To further validate the biological significance of the three binding motifs we determined the frequency of each sequence in a dataset of genes upregulated in the brains of HuD overexpressor mice (HuD-Tg). As described previously, HuD-Tg mice have increased levels of HuD in neurons of the forebrain (14) and increased levels of GAP-43 and AChE mRNAs, two well characterized HuD targets (14,19). Microarray gene expression analysis of the HuD-Tg mice forebrain identified 646 probe sets representing 419 transcripts that had a 'present' call and whose expression was significantly upregulated in these mice ($P < 0.05$, *t*-test). Sequence analyses of this set of mRNAs revealed that the frequency of the three motifs (motif 1, 36.3%; motif 2, 36.3% and motif 3, 21.2%) was significantly increased in their 3′ UTRs (Figure 5). Also, we found that the 5′ UTRs of upregulated mRNAs had increased frequencies of motif 1 but decreased frequencies of motifs 2 and 3. Finally, our finding that many upregulated transcripts did not contain HuD-binding motifs suggest that some of the

Table 2. Characteristics of the datasets used in the present studies

	5′ UTR				CR				3′ UTR			
	Genome	Chip	Forebrain	HuD targets	Genome	Chip	Forebrain	HuD targets	Genome	Chip	Forebrain	HuD Targets
Number of sequences	12 397	11 036	8200	421	23 679	19 029	8688	608	17 918	16 359	8363	572
Length	380	367	274	359	1469	1605	1739	1593	1121	1142	1325	1,909
A	20.48	19.92	17.97	18.3	25.52	25.5	25.97	27.63	26.6	26.45	26.39	27.86
U	20.12	19.7	17.93	18.85	22.8	21.95	21.66	22.68	28.76	28.74	29.28	32.95
C	29.23	29.67	30.77	30.9	25.73	25.97	25.52	23.92	22.55	22.65	22.27	19.11
G	30.18	30.71	33.34	31.95	25.95	26.58	26.85	25.77	22.08	22.16	22.06	20.08

3′ UTR sequences were retrieved from Ensembl BioMart and datasets were made non-redundant by Gene ID. The datasets were analyzed by scripts written in Perl v5.8.8 and using BioPerl modules.

Table 3. Predicted location of HuD-binding motifs in selected known and new HuD targets

mRNA	Motif 1	Motif 2	Motif 3
Known HuD targets			
GAP-43	128 332	–	–
MARCKS	518 522 526 530 534 538 542 546	151 158 275 276 277 278 279	111 559 560
Neuroserpin	1801 1803 1805 1807 1809 1811 1813 1815 1817 1819 1821 1823 1825 1827 1829 1831 1833 1835 1837 1839 1841 1843	2073	615
N-myc	–	–	244 245 369
p21 waf1	133 1211	–	–
tau	–	–	–
VEGF	939 1261	–	397
p27 5UTR	225 233 306	436	–
p27 3UTR	–	878 879 880 881 882 883 884 885 886 887 888 889	475 597 891
New HuD targets			
eIF4e	–	563 657	–
HuR	–	1190 1199	–
HuB	–	456	–
Fkbp1a	976	–	–
PPP1cb	985	–	–
PPP3ca	–	15	–
CaMkinIIα	1475 1483 1485 1487 1491 1497 1512 3032 3034 3036 3038 3040 3042 3044 3046 3048 3050 3052 3054 3056 3058 3060 3062 3064 3066 3068 3070	3294 3298 3302 3306 3312	–
Homer1	–	–	754
Rab1	891 1247 1249	–	–
N-CAM1	75 77 79 81 83	744 1108 1109 1317 1334 1351 1352 1353 1354 1355 1356 1357 1358 1359 2833 2837	2705
Musashi 2	274 276 280	253 416 421 422 426 456 461 1558 1563 1570 1575 1764 1765 2258 2263 2760 3632 3638 3889 4248 4253	1141 1580 1767 1768 1871 1872 2955 2956 3642 4082 4083

The predicted location of each motif in the 3′ UTR of selected HuD targets. As described in the 'Materials and Methods' section, Pearl scripts were used to search for the location of each motif, allowing one mismatch in each consensus sequence.

observed gene expression changes are indirect events regulated by HuD targets rather that direct HuD effects, which is expected in animals with constitutive HuD overexpression.

Gene ontology analysis of HuD targets

It has been proposed that mRNAs coordinately regulated by the same RBP comprise a post-transcriptional operon or 'RNA regulon' (49). To gain a further understanding of the biological processes regulated by HuD, subsequent studies examined the Gene Ontology distribution of HuD targets (Figure 6). Several gene ontology categories were significantly enriched in HuD targets relative to the genome. Amongst these categories were axon guidance and regulation of neuron differentiation, two processes that are known to be regulated by HuD in several models. Other biological processes that were targeted by

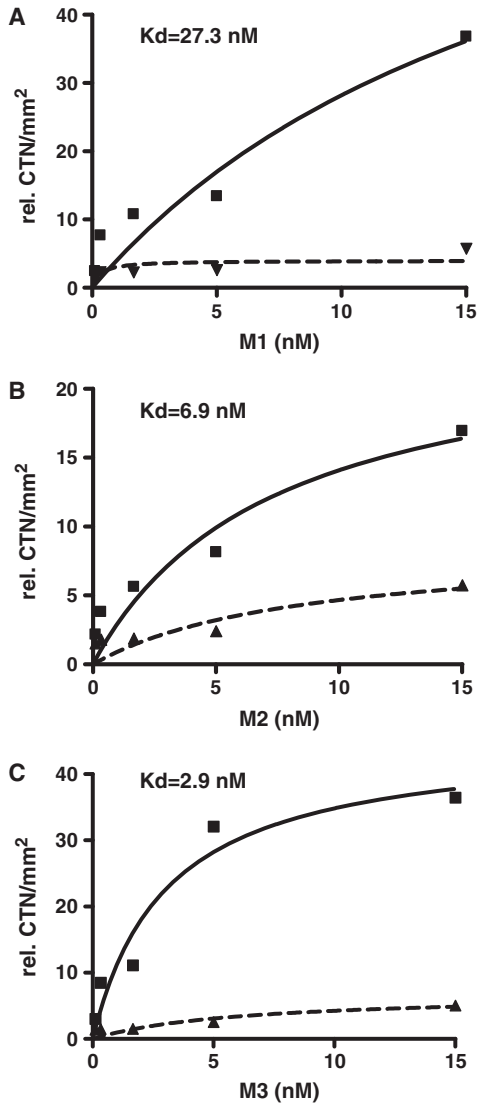

Figure 4. Binding affinities of recombinant HuD for the three motifs. Panels show binding curves of motif 1 (**A**), motif 2 (**B**) and motif 3 (**C**). In vitro binding assays were performed with increasing amounts of radiolabeled oligoribonucleotides corresponding to the most likely sequence in each motif (CCCUCCCUCUCUC for motif 1, UUUUG UUUUGUUU for motif 2 and UUUUUUUUUUAAA for motif 3) and fixed amounts GST-HuD as indicated in 'Materials and Methods' section. Non-specific binding was measured using a 100 molar excess of cold oligoribonucleotides. Binding curves of total (solid line) and non-specific (dashed lines) used to calculate the K_d for each motifs.

HuD were unexpected such as regulation of translation initiation, RNA processing, and protein amino acid dephosphorylation. Likewise, we found that molecular categories such as RNA-binding, protein phosphatase activity type 1 activity, GTP-binding and actin-binding were significantly enriched in HuD targets. Analysis of cellular components revealed that lamellipodium, actin cytoskeleton and ribonucleoprotein complex, all components related to growth cone activity and axonal growth as well as neural plasticity, were significantly overpopulated with HuD targets. Finally, to put the set of HuD targets in a biological context we searched for canonical cellular pathways containing multiple targets. Among these, we found that the developmental wnt signaling pathway and the long-term potentiation pathway contain a number of HuD targets (Supplementary Figure S2). Likewise, analysis of cellular networks using Metacore software revealed that several networks such as those centered on β-actin and the translation factor eIF4E (Supplementary Figure 3) were overpopulated by HuD targets. These examples highlight the importance of HuD in the post-transcriptional control of gene regulation during neural development and synaptic plasticity.

DISCUSSION

The identification of the host of cellular targets regulated by specific RBPs is critical for understanding the biological function of these regulatory proteins. In this study, we used a two-step mRNA–RBP complex purification method and genome-wide bioinformatics analyses to identify the targets of the ELAV-like protein HuD, define its recognition motifs and characterize the cellular pathways regulated by this protein. HuD is expressed in neurons where it promotes axonal growth during nervous system development and participates in synaptic plasticity mechanisms in the mature brain (15,17,20,21,50–53). Not only is HuD present in neuronal cell bodies (14,18), but it is also localized to growth cones (54) and dendrites (51), two regions whereby neurons communicate with each other and the environment and sites of local post-transcriptional regulation (55,56). Consistent with the known functions of HuD, we found that its target mRNAs encoded proteins involved in processes critical for neuronal differentiation such as axon guidance, actin reorganization and wnt signaling. In addition, HuD targets were found to participate in novel pathways such as protein phosphatase regulation, ubiquitin ligation and mRNA transport, processing and translation.

The methods used to isolate mRNAs bound to RNA-BPs typically utilize either immunoprecipitation of RNA–protein complexes, with or without prior cross-linking, or *in vitro* pull down assays of purified RNA with recombinant RNA-BPs. The problem with the latter method is that it does not take into consideration that mRNAs that interact *in vitro* with specific RNA-BPs may never do so *in vivo* as they could be localized to different subcellular fractions or different cell types in the tissue. To avoid this problem, Keene and colleagues devised a method to isolate mRNP complexes under conditions that preserve *in vivo* RNA-protein interactions (25,26). Given that HuD is known to interact with other RBPs including other members of the Hu protein family (30–32), it is possible that some of the mRNAs in the initial IP could be bound to other protein in the mRNP. Therefore, to isolate directly bound mRNAs, transcripts in the HuD IP were further purified using *in vitro* pull downs with recombinant protein and HuD targets were defined as the mRNAs with highest enrichment values. On average, HuD targets were found to contain longer 3′ UTRs comprising an increased proportion of ARE sequences and HuD-binding motifs. These motifs were also significantly enriched in a dataset of mRNAs

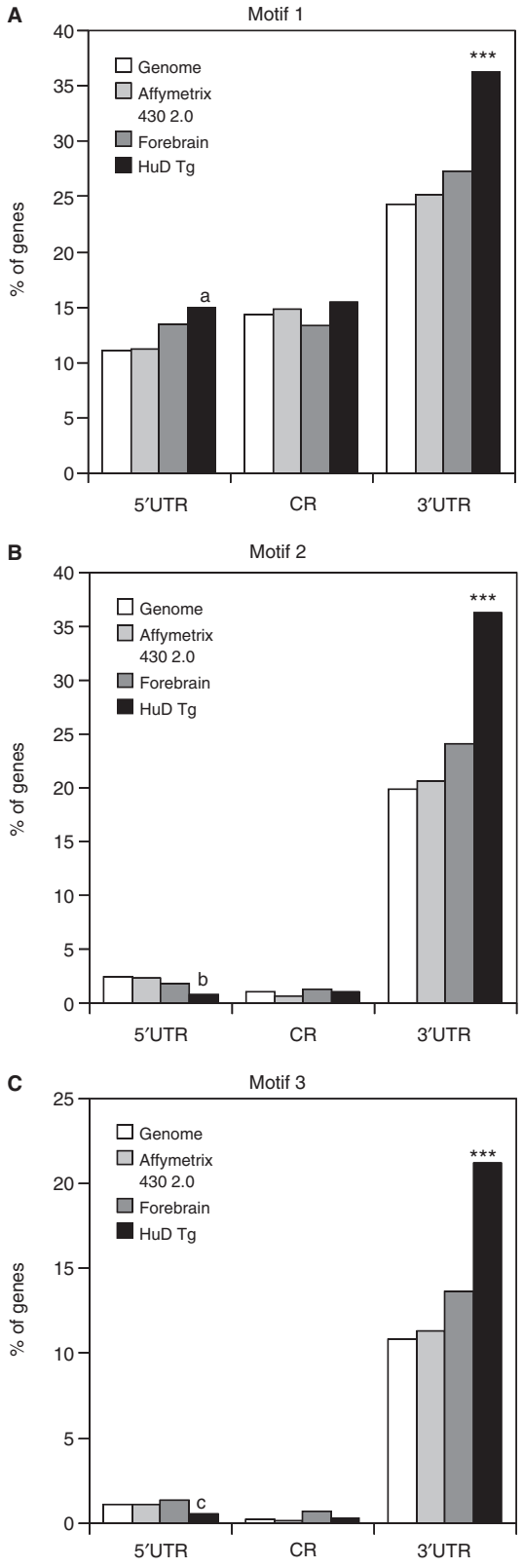

Figure 5. Increased frequency of HuD-binding motifs in mRNAs upregulated in the brains of HuD overexpressor mice. (**A**) Frequency of HuD-binding motif 1 in the 5′ UTR, CR and 3′ UTR of mouse genome (white bars), Affymetrix 430 2.0 chip genes (light grey bars), forebrain transcripts (dark grey bars) and mRNAs upregulated in HuD-Tg mice (black bars). (**B**) Same analysis for HuD-binding motif 2. (**C**) Frequency of motif 3 in the same gene datasets. ***$P < 0.0001$ HuD-Tg mice versus each of the three reference sets (genome, chip and forebrain), (a) $P < 0.02$ versus genome and chip, (b) $P < 0.05$ versus genome and chip and (c) $P < 0.05$ versus all three reference sets.

upregulated in the forebrain of HuD overexpressor mice, validating the biological significance of these sequences.

All four ELAV-like Hu proteins have been shown to interact with ARE sequences via their first and second RRMs, while the third RRM binds to long poly A tails (57,58). Previous predictions of Hu protein binding motifs have been based upon the consensus sequences of target mRNAs (27,59). In addition to this criterion, in this study, we took advantage of the known crystal structure of the complex of HuD's RRM I and II and Type I AREs and restricted our search to motifs that matched its seven nucleotide (YUNNYUY) minimal consensus sequence (34). Based on this sequence restriction and the 3′ UTR sequences of the most enriched targets, three new HuD recognition motifs were identified. Consistent with the ARE-binding motifs of other ELAV-like proteins (27,59), two of the HuD-binding motifs (motifs 2 and 3) are U-rich; with motif 2 having interspersed Gs similar to the sex-lethal binding site (47) and the recently identified GRE (9) and motif 3 matching class I and II ARE sequences. HuD was found to bind with high affinity to ribo-oligonucleotides containing motifs 2 and 3 sequences. In contrast, binding to motif 1, which is C-rich with interspersed Us, was about one order of magnitude lower than that of motif 3. Although none of the ELAV-binding proteins were shown to recognize pure C sequences, HuR was found to interact with a CU-rich element in the androgen receptor mRNA (46).

Analysis of the distribution of all three HuD-binding motifs in target mRNAs showed that these sequences were primarily localized to the 3′ UTR. Interestingly, these motifs were also present at higher frequencies in the 5′ UTRs of target mRNAs. Although the vast majority of instability conferring sequences described so far mapped to the 3′ UTR, a few of them were found in the 5′ UTR and coding region (10,11). Furthermore, for at least one mRNA, that encoding the cdk inhibitor p27, HuD binds to an IRES like sequence in its 5′ UTR repressing translation (48). As shown in Table 3, we found several putative HuD-binding motifs in both the 5′ UTR and 3′ UTRs of p27 mRNA. In addition to HuD, HuB was shown to increase translation of neurofilament M (60) and HuR to block translation of IGF-I receptor (61). Finally, not only is HuD co-localized with ribosomes in neuronal cell bodies (18), growth cones (54) and dendrites (51) but it also, as shown by a recent study, co-localizes with two important translational regulators, the poly(A)-binding protein (PABP) and the cap-binding protein (eIF4E) (62). Altogether, these results suggest that in addition to controlling mRNA stability, in some instances HuD and other Hu proteins could also regulate the rate of translation of specific mRNAs by interacting with sequences in the 5′ UTR.

Gene ontology and biological pathway analyses of putative HuD targets revealed several interesting

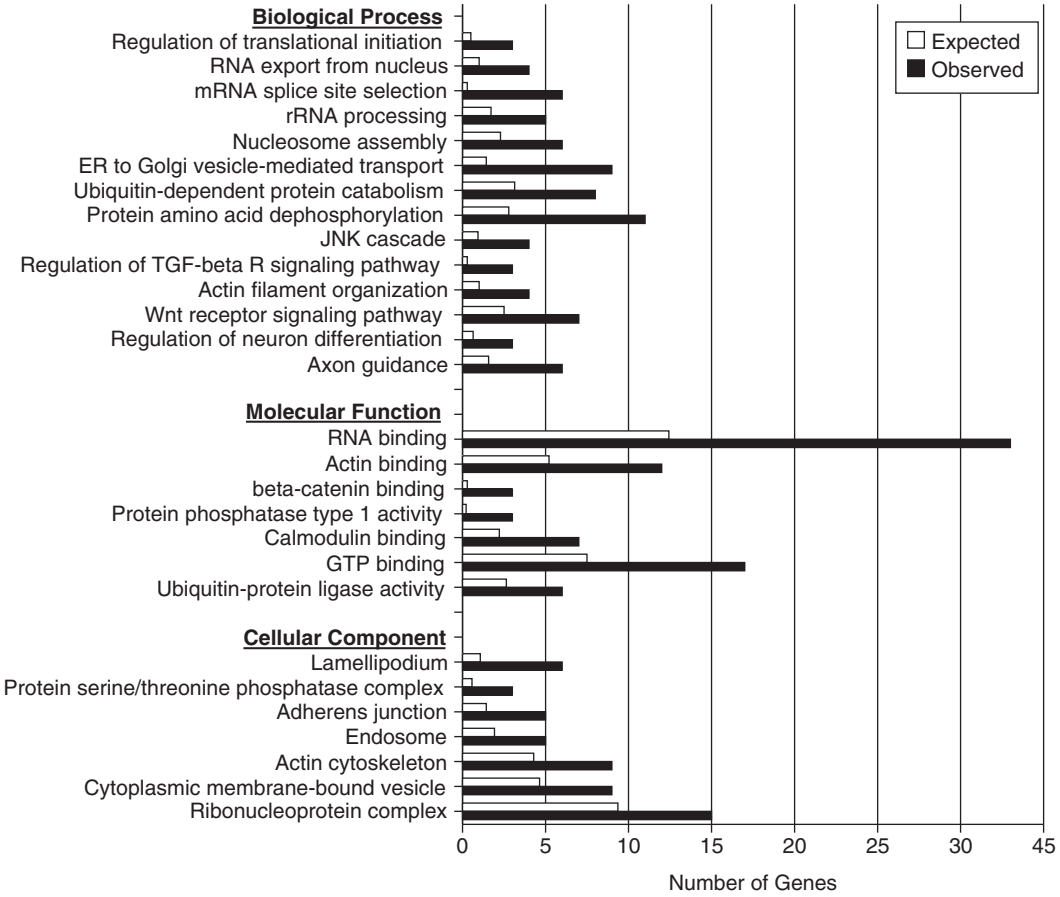

Figure 6. Gene Ontology analysis of HuD targets. The graph shows the number of HuD target genes observed in each gene ontology category (black bars) and the expected number in the genome (white bars). All the categories presented in the graph have *P*-values < 0.01.

features of this dataset. For instance, ~7% of HuD targets were other RBPs, including HuD itself, HuB, HuR, polypyrimidine tract binding protein 2 (Ptbp2), CUG triplet repeat-binding protein 2 (Cugbp2), cytoplasmic polyadenylation element binding protein 3 (Cpeb3), poly(rC) binding protein 2 (Pcbp2), Pumillio 2, Staufen 2, Musashi 2 as well as several hnRNP proteins and splicing factors. Our finding that HuD binds its own mRNA and those of other ELAV-like proteins is similar to that observed for Drosophila ELAV, which has been shown to bind and downregulate the expression of its own mRNA (63). These findings also correlate with the decreases in HuB and HuR mRNAs observed in the brains of our HuD overexpressor mice (14). Likewise, HuR was shown to associate with its cognate mRNA and with mRNAs encoding other RBPs (40,64). Additional clues on the importance of HuD in gene regulation comes from our findings that HuD targets also encode proteins controlling translational initiation, RNA export from the nucleus, mRNA splice site selection and nucleosome assembly (Figure 6). These observations support a model in which HuD and other RNA-BPs form a complex and highly integrated network of post-transcriptional regulators.

In agreement with the role of HuD in neural development and axonal outgrowth (24,53,65–68), gene ontology analyses also revealed that multiple HuD targets are associated with axon guidance and related processes such as regulation of actin dynamics and vesicle trafficking. Furthermore, other important developmental pathways such as those involving wnt, TGF-β and β-catenin signaling are also overpopulated with HuD targets. Finally, concurring with the known biological properties of HuD and other Hu proteins in synaptic plasticity (20,21) many HuD targets encode proteins implicated in these processes. For instance, HuD targets include protein phosphatases such as PPP1 and PPP3 (aka PP2B or calcineurin) and a regulator of PPP3 activity (FKBP1 a.k.a., FKB12), which are known to participate in long-term potentiation and long-term depression, two different forms of synaptic plasticity (69). Additionally, another HuD target, the metabotropic glutamate receptor 5 (mGluR5), is known to control localized protein synthesis in dendrites during activity-dependent synaptic remodeling (70). Along these lines, two recent studies demonstrated the activity-dependent transport of HuD to neuronal processes and corresponding increased binding of HuD to the mRNAs for the plasticity associated proteins homer 1a, GAP-43 and CaMKinIIα (62,71).

In conclusion, our results demonstrate that the ELAV-like protein HuD binds to three novel motifs in the 3′

UTRs of its target mRNAs and that multiple HuD targets encode proteins involved in post-transcriptional gene regulation, neuronal differentiation and synaptic remodeling. These findings support a post-transcriptional operon model in which HuD interacts with multiple mRNAs to regulate these complex biological processes.

SUPPLEMENTARY DATA

Supplementary Data are available at NAR Online.

ACKNOWLEDGEMENTS

The authors thank Dr Rebecca Hartley for critical reading of the manuscript and Dr Jack Keene and Neel Mukherjee for their help with the IP data analyses.

FUNDING

National Institutes of Health (grant number NS30255 to N.P.B.). Funding for open access charge: National Institutes of Health (grant NS30255 to N.P.B.).

Conflict of interest statement. None declared.

REFERENCES

1. Wilusz,C.J., Wormington,M. and Peltz,S.W. (2001) The cap-to-tail guide to mRNA turnover. *Nat. Rev. Mol. Cell Biol.*, **2**, 237–246.
2. Bolognani,F. and Perrone-Bizzozero,N.I. (2008) RNA-protein interactions and control of mRNA stability in neurons. *J. Neurosci. Res.*, **86**, 481–489.
3. Bartel,D.P. (2004) MicroRNAs: genomics, biogenesis, mechanism, and function. *Cell*, **116**, 281–297.
4. Shaw,G. and Kamen,R. (1986) A conserved AU sequence from the 3′ untranslated region of GM-CSF mRNA mediates selective mRNA degradation. *Cell*, **46**, 659–667.
5. Chen,C.Y. and Shyu,A.B. (1995) AU-rich elements: characterization and importance in mRNA degradation. *Trends Biochem. Sci.*, **20**, 465–470.
6. Bakheet,T., Williams,B.R. and Khabar,K.S. (2006) ARED 3.0: the large and diverse AU-rich transcriptome. *Nucleic Acids Res.*, **34**, D111–D114.
7. Marquis,J., Paillard,L., Audic,Y., Cosson,B., Danos,O., Le Bec,C. and Osborne,H.B. (2006) CUG-BP1/CELF1 requires UGU-rich sequences for high-affinity binding. *Biochem. J.*, **400**, 291–301.
8. Moraes,K.C., Wilusz,C.J. and Wilusz,J. (2006) CUG-BP binds to RNA substrates and recruits PARN deadenylase. *RNA*, **12**, 1084–1091.
9. Vlasova,I.A., Tahoe,N.M., Fan,D., Larsson,O., Rattenbacher,B., Sternjohn,J.R., Vasdewani,J., Karypis,G., Reilly,C.S., Bitterman,P.B. *et al.* (2008) Conserved GU-rich elements mediate mRNA decay by binding to CUG-binding protein 1. *Mol. Cell*, **29**, 263–270.
10. Chen,C.Y., Del Gatto-Konczak,F., Wu,Z. and Karin,M. (1998) Stabilization of interleukin-2 mRNA by the c-Jun NH2-terminal kinase pathway. *Science*, **280**, 1945–1949.
11. Grosset,C., Chen,C.Y., Xu,N., Sonenberg,N., Jacquemin-Sablon,H. and Shyu,A.B. (2000) A mechanism for translationally coupled mRNA turnover: interaction between the poly(A) tail and a c-fos RNA coding determinant via a protein complex. *Cell*, **103**, 29–40.
12. Szabo,A., Dalmau,J., Manley,G., Rosenfeld,M., Wong,E., Henson,J., Posner,J.B. and Furneaux,H.M. (1991) HuD, a paraneoplastic encephalomyelitis antigen, contains RNA-binding domains and is homologous to Elav and Sex-lethal. *Cell*, **67**, 325–333.
13. Akamatsu,W., Fujihara,H., Mitsuhashi,T., Yano,M., Shibata,S., Hayakawa,Y., Okano,H.J., Sakakibara,S., Takano,H., Takano,T. *et al.* (2005) The RNA-binding protein HuD regulates neuronal cell identity and maturation. *Proc. Natl Acad. Sci. USA*, **102**, 4625–4630.
14. Bolognani,F., Tanner,D.C., Merhege,M., Deschenes-Furry,J., Jasmin,B. and Perrone-Bizzozero,N.I. (2006) In vivo post-transcriptional regulation of GAP-43 mRNA by overexpression of the RNA-binding protein HuD. *J. Neurochem.*, **96**, 790–801.
15. Bolognani,F., Tanner,D.C., Nixon,S., Okano,H.J., Okano,H. and Perrone-Bizzozero,N.I. (2007) Coordinated expression of HuD and GAP-43 in hippocampal dentate granule cells during developmental and adult plasticity. *Neurochem. Res.*, **32**, 2142–2151.
16. Tanner,D.C., Qiu,S., Bolognani,F., Partridge,L.D., Weeber,E.J. and Perrone-Bizzozero,N.I. (2008) Alterations in mossy fiber physiology and GAP-43 expression and function in transgenic mice overexpressing HuD. *Hippocampus*, **18**, 814–823.
17. Bolognani,F., Qiu,S., Tanner,D.C., Paik,J., Perrone-Bizzozero,N.I. and Weeber,E.J. (2007) Associative and spatial learning and memory deficits in transgenic mice overexpressing the RNA-binding protein HuD. *Neurobiol. Learn. Mem.*, **87**, 635–643.
18. Anderson,K.D., Merhege,M.A., Morin,M., Bolognani,F. and Perrone-Bizzozero,N.I. (2003) Increased expression and localization of the RNA-binding protein HuD and GAP-43 mRNA to cytoplasmic granules in DRG neurons during nerve regeneration. *Exp. Neurol.*, **183**, 100–108.
19. Deschenes-Furry,J., Mousavi,K., Bolognani,F., Neve,R.L., Parks,R.J., Perrone-Bizzozero,N.I. and Jasmin,B.J. (2007) The RNA-binding protein HuD binds acetylcholinesterase mRNA in neurons and regulates its expression after axotomy. *J. Neurosci.*, **27**, 665–675.
20. Perrone-Bizzozero,N. and Bolognani,F. (2002) Role of HuD and other RNA-binding proteins in neural development and plasticity. *J. Neurosci. Res.*, **68**, 121–126.
21. Pascale,A., Amadio,M. and Quattrone,A. (2008) Defining a neuron: neuronal ELAV proteins. *Cell Mol. Life Sci.*, **65**, 128–140.
22. Chung,S., Eckrich,M., Perrone-Bizzozero,N., Kohn,D.T. and Furneaux,H. (1997) The Elav-like proteins bind to a conserved regulatory element in the 3′-untranslated region of GAP-43 mRNA. *J. Biol. Chem.*, **272**, 6593–6598.
23. Beckel-Mitchener,A.C., Miera,A., Keller,R. and Perrone-Bizzozero,N.I. (2002) Poly(A) tail length-dependent stabilization of GAP-43 mRNA by the RNA-binding protein HuD. *J. Biol. Chem.*, **277**, 27996–28002.
24. Anderson,K.D., Morin,M.A., Beckel-Mitchener,A., Mobarak,C.D., Neve,R.L., Furneaux,H.M., Burry,R. and Perrone-Bizzozero,N.I. (2000) Overexpression of HuD, but not of its truncated form HuD I+II, promotes GAP-43 gene expression and neurite outgrowth in PC12 cells in the absence of nerve growth factor. *J. Neurochem.*, **75**, 1103–1114.
25. Tenenbaum,S.A., Carson,C.C., Lager,P.J. and Keene,J.D. (2000) Identifying mRNA subsets in messenger ribonucleoprotein complexes by using cDNA arrays. *Proc. Natl Acad. Sci. USA*, **97**, 14085–14090.
26. Tenenbaum,S.A., Lager,P.J., Carson,C.C. and Keene,J.D. (2002) Ribonomics: identifying mRNA subsets in mRNP complexes using antibodies to RNA-binding proteins and genomic arrays. *Methods*, **26**, 191–198.
27. Lopez de Silanes,I., Zhan,M., Lal,A., Yang,X. and Gorospe,M. (2004) Identification of a target RNA motif for RNA-binding protein HuR. *Proc. Natl Acad. Sci. USA*, **101**, 2987–2992.
28. Halbeisen,R.E., Galgano,A., Scherrer,T. and Gerber,A.P. (2008) Post-transcriptional gene regulation: from genome-wide studies to principles. *Cell Mol. Life Sci.*, **65**, 798–813.
29. Keene,J.D. and Tenenbaum,S.A. (2002) Eukaryotic mRNPs may represent posttranscriptional operons. *Mol. Cell*, **9**, 1161–1167.
30. Kasashima,K., Sakashita,E., Saito,K. and Sakamoto,H. (2002) Complex formation of the neuron-specific ELAV-like Hu RNA-binding proteins. *Nucleic Acids Res.*, **30**, 4519–4526.
31. Saito,K., Fujiwara,T., Katahira,J., Inoue,K. and Sakamoto,H. (2004) TAP/NXF1, the primary mRNA export receptor, specifically interacts with a neuronal RNA-binding protein HuD. *Biochem. Biophys. Res. Commun.*, **321**, 291–297.
32. Atlas,R., Behar,L., Elliott,E. and Ginzburg,I. (2004) The insulin-like growth factor mRNA binding-protein IMP-1 and the

Ras-regulatory protein G3BP associate with tau mRNA and HuD protein in differentiated P19 neuronal cells. *J. Neurochem.*, **89**, 613–626.
33. Chung,S., Jiang,L., Cheng,S. and Furneaux,H. (1996) Purification and properties of HuD, a neuronal RNA-binding protein. *J. Biol. Chem.*, **271**, 11518–11524.
34. Wang,X. and Tanaka Hall,T.M. (2001) Structural basis for recognition of AU-rich element RNA by the HuD protein. *Nat. Struct. Biol.*, **8**, 141–145.
35. Bailey,T.L. and Gribskov,M. (1998) Combining evidence using p-values: application to sequence homology searches. *Bioinformatics*, **14**, 48–54.
36. Bailey,T.L., Williams,N., Misleh,C. and Li,W.W. (2006) MEME: discovering and analyzing DNA and protein sequence motifs. *Nucleic Acids Res.*, **34**, W369–W373.
37. Crooks,G.E., Hon,G., Chandonia,J.M. and Brenner,S.E. (2004) WebLogo: a sequence logo generator. *Genome Res.*, **14**, 1188–1190.
38. Zhang,B., Schmoyer,D., Kirov,S. and Snoddy,J. (2004) GOTree Machine (GOTM): a web-based platform for interpreting sets of interesting genes using Gene Ontology hierarchies. *BMC Bioinformatics*, **5**, 16.
39. Zhang,B., Kirov,S. and Snoddy,J. (2005) WebGestalt: an integrated system for exploring gene sets in various biological contexts. *Nucleic Acids Res.*, **33**, W741–W748.
40. Mukherjee,N., Lager,P.J., Freidersdorf,M., Thompson,M. and Keene,J.D. (2009) Coordinated posttranscriptional mRNA population dynamics during T-Cell activation. *Mol. Syst. Biol.*, **5**, 288. Epub 28 July 2009.
41. Okazaki,N., Imai,K., Kikuno,R.F., Misawa,K., Kawai,M., Inamoto,S., Ohara,R., Nagase,T., Ohara,O. and Koga,H. (2005) Influence of the 3′-UTR-length of mKIAA cDNAs and their sequence features to the mRNA expression level in the brain. *DNA Res.*, **12**, 181–189.
42. Wedgwood,S., Lam,W.K., Pinchin,K.M., Markham,A.F., Cartwright,E.J. and Coletta,P.L.Mamm. (2000) Characterization of a brain-selective transcript of the Adenomatous polyposis coli tumor suppressor gene. *Genome*, **11**, 1150–1153.
43. Suda,S., Nibuya,M., Suda,H., Takamatsu,K., Miyazaki,T., Nomura,S. and Kawai,N. (2002) Potassium channel mRNAs with AU-rich elements and brain-specific expression. *Biochem. Biophys. Res. Commun.*, **291**, 1265–1271.
44. Pelka,G.J., Watson,C.M., Christodoulou,J. and Tam,P.P. (2005) Distinct expression profiles of Mecp2 transcripts with different lengths of 3′UTR in the brain and visceral organs during mouse development. *Genomics*, **85**, 441–452.
45. Kong,J., Ji,X. and Liebhaber,S.A. (2003) The KH-domain protein alpha CP has a direct role in mRNA stabilization independent of its cognate binding site. *Mol. Cell Biol.*, **23**, 1125–1134.
46. Yeap,B.B., Voon,D.C., Vivian,J.P., McCulloch,R.K., Thomson,A.M., Giles,K.M., Czyzyk-Krzeska,M.F., Furneaux,H., Wilce,M.C., Wilce,J.A. *et al.* (2002) Novel binding of HuR and poly(C)-binding protein to a conserved UC-rich motif within the 3′-untranslated region of the androgen receptor messenger RNA. *J. Biol. Chem.*, **277**, 27183–27192.
47. Handa,N., Nureki,O., Kurimoto,K., Kim,I., Sakamoto,H., Shimura,Y., Muto,Y. and Yokoyama,S. (1999) Structural basis for recognition of the tra mRNA precursor by the sex-lethal protein. *Nature*, **398**, 579–585.
48. Kullmann,M., Gopfert,U., Siewe,B. and Hengst,L. (2002) ELAV/Hu proteins inhibit p27 translation via an IRES element in the p27 5′UTR. *Genes Dev.*, **16**, 3087–3099.
49. Keene,J.D. (2007) RNA regulons: coordination of post-transcriptional events. *Nat. Rev. Genet.*, **8**, 533–543.
50. Quattrone,A., Pascale,A., Nogues,X., Zhao,W., Gusev,P., Pacini,A. and Alkon,D.L. (2001) Posttranscriptional regulation of gene expression in learning by the neuronal ELAV-like mRNA-stabilizing proteins. *Proc. Natl Acad. Sci. USA*, **98**, 11668–11673.
51. Bolognani,F., Merhege,M.A., Twiss,J. and Nora,I.P.-B. (2004) Dendritic localization of the RNA-binding protein HuD in hippocampal neurons: association with polysomes and upregulation during contextual learning. *Neurosci. Lett.*, **371**, 152–157.
52. Pascale,A., Gusev,P.A., Amadio,M., Dottorini,T., Govoni,S., Alkon,D.L. and Quattrone,A. (2004) Increase of the RNA-binding protein HuD and posttranscriptional up-regulation of the GAP-43 gene during spatial memory. *Proc. Natl Acad. Sci. USA*, **101**, 1217–1222.
53. Anderson,K.D., Sengupta,J., Morin,M., Neve,R.L., Valenzuela,C.F. and Perrone-Bizzozero,N.I. (2001) Overexpression of HuD accelerates neurite outgrowth and increases GAP-43 mRNA expression in cortical neurons and retinoic acid-induced embryonic stem cells in vitro. *Exp. Neurol.*, **168**, 250–258.
54. Smith,C.L., Afroz,R., Bassell,G.J., Furneaux,H.M., Perrone-Bizzozero,N.I. and Burry,R.W. (2004) GAP-43 mRNA in growth cones is associated with HuD and ribosomes. *J. Neurobiol.*, **61**, 222–235.
55. Giuditta,A., Chun,J.T., Eyman,M., Cefaliello,C., Bruno,A.P. and Crispino,M. (2008) Local gene expression in axons and nerve endings: the glia-neuron unit. *Physiol. Rev.*, **88**, 515–555.
56. Zeitelhofer,M., Macchi,P. and Dahm,R. (2008) Perplexing bodies: the putative roles of P-bodies in neurons. *RNA Biol.*, **5**, 244–248.
57. Abe,R., Sakashita,E., Yamamoto,K. and Sakamoto,H. (1996) Two different RNA binding activities for the AU-rich element and the poly(A) sequence of the mouse neuronal protein mHuC. *Nucleic Acids Res.*, **24**, 4895–4901.
58. Ma,W.J., Chung,S. and Furneaux,H. (1997) The Elav-like proteins bind to AU-rich elements and to the poly(A) tail of mRNA. *Nucleic Acids Res.*, **25**, 3564–3569.
59. Gao,F.B., Carson,C.C., Levine,T. and Keene,J.D. (1994) Selection of a subset of mRNAs from combinatorial 3′ untranslated region libraries using neuronal RNA-binding protein Hel-N1. *Proc. Natl Acad. Sci. USA*, **91**, 11207–11211.
60. Antic,D., Lu,N. and Keene,J.D. (1999) ELAV tumor antigen, Hel-N1, increases translation of neurofilament M mRNA and induces formation of neurites in human teratocarcinoma cells. *Genes Dev.*, **13**, 449–461.
61. Meng,Z., King,P.H., Nabors,L.B., Jackson,N.L., Chen,C.Y., Emanuel,P.D. and Blume,S.W. (2005) The ELAV RNA-stability factor HuR binds the 5′-untranslated region of the human IGF-IR transcript and differentially represses cap-dependent and IRES-mediated translation. *Nucleic Acids Res.*, **33**, 2962–2979.
62. Tiruchinapalli,D.M., Ehlers,M.D. and Keene,J.D. (2008) Activity-dependent expression of RNA binding protein HuD and its association with mRNAs in neurons. *RNA Biol.*, **5**, 157–168.
63. Samson,M.L. (1998) Evidence for 3′ untranslated region-dependent autoregulation of the Drosophila gene encoding the neuronal nuclear RNA-binding protein ELAV. *Genetics*, **150**, 723–733.
64. Pullmann,R. Jr, Kim,H.H., Abdelmohsen,K., Lal,A., Martindale,J.L., Yang,X. and Gorospe,M. (2007) Analysis of turnover and translation regulatory RNA-binding protein expression through binding to cognate mRNAs. *Mol. Cell Biol.*, **27**, 6265–6278.
65. Okano,H.J. and Darnell,R.B. (1997) A hierarchy of Hu RNA binding proteins in developing and adult neurons. *J. Neurosci.*, **17**, 3024–3037.
66. Dobashi,Y., Shoji,M., Wakata,Y. and Kameya,T. (1998) Expression of HuD protein is essential for initial phase of neuronal differentiation in rat pheochromocytoma cells. *Biochem. Biophys. Res. Commun.*, **244**, 226–229.
67. Kasashima,K., Terashima,K., Yamamoto,K., Sakashita,E. and Sakamoto,H. (1999) Cytoplasmic localization is required for the mammalian ELAV-like protein HuD to induce neuronal differentiation. *Genes Cells*, **4**, 667–683.
68. Mobarak,C.D., Anderson,K.D., Morin,M., Beckel-Mitchener,A., Rogers,S.L., Furneaux,H., King,P. and Perrone-Bizzozero,N.I. (2000) The RNA-binding protein HuD is required for GAP-43 mRNA stability, GAP-43 gene expression, and PKC-dependent neurite outgrowth in PC12 cells. *Mol. Biol. Cell*, **11**, 3191–3203.
69. Winder,D.G. and Sweatt,J.D. (2001) Roles of serine/threonine phosphatases in hippocampal synaptic plasticity. *Nat. Rev. Neurosci.*, **2**, 461–474.
70. Huber,K.M., Roder,J.C. and Bear,M.F. (2001) Chemical induction of mGluR5- and protein synthesis–dependent long-term depression in hippocampal area CA1. *J. Neurophysiol.*, **86**, 321–325.
71. Tiruchinapalli,D.M., Caron,M.G. and Keene,J.D. (2008a) Activity-dependent expression of ELAV/Hu RBPs and neuronal mRNAs in seizure and cocaine brain. *J. Neurochem.*, **107**, 1529–1543.